

# Intramolecular Fluorescence Quenching of Tyrosine by the Peptide $\alpha$ -Carbonyl Group Revisited

Melinda Noronha,<sup>†</sup> João C. Lima,<sup>‡</sup> Pedro Lamosa,<sup>†</sup> Helena Santos,<sup>†</sup> Christopher Maycock,<sup>†</sup> Rita Ventura,<sup>†</sup> and António L. Maçanita<sup>\*,§</sup>

*Instituto de Tecnologia Química e Biológica, Universidade Nova de Lisboa, Rua da Quinta Grande 6, Apartado 127, 2780-156 Oeiras, Portugal, REQUIMTE/CQFB, Faculdade de Ciências e Tecnologia, Universidade Nova de Lisboa, Quinta da Torre, Monte de Caparica, 2829-516 Caparica, and Departamento de Química, Instituto Superior Técnico, Universidade Técnica de Lisboa, 1049-001 Lisboa, Portugal*

Received: October 15, 2003; In Final Form: January 6, 2004

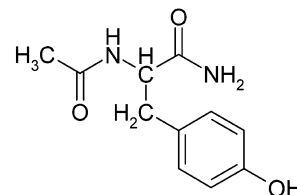
The environment-dependent multiexponential behavior of *N*-acetyltyrosinamide (NAYA) and other tyrosine derivatives is revisited, aiming for a better understanding of tyrosine as an intrinsic fluorescent probe for protein microenvironment changes during conformational changes. The effects of solvent polarity, viscosity, and temperature on the fluorescence decay of NAYA were evaluated using dioxane–water mixtures and pure solvents. Double-exponential decays were observed in dioxane–water mixtures above 70% (v/v) water concentration including pure water, for temperatures below 50 °C. However, at higher temperatures, or in dioxane–water mixtures with lower water concentrations, NAYA shows single-exponential decays. Single-exponential decays were also generally observed in pure solvents (dioxane, acetonitrile, methanol, ethanol, DMSO). The exception was the strong hydrogen-bond donor trifluoroethanol, in which NAYA decays as a double exponential. The results are consistent with a solvent-modulated excited-state intramolecular electron transfer from the phenol to the amide moiety occurring in one of the three rotamers of NAYA. On the basis of a full kinetic analysis of the data, it is shown that experimental observation of double-exponential decays depends on three factors: the ground-state population of rotamers, their rates of interconversion ( $k_r = 4.4 \times 10^8 \text{ s}^{-1}$  and  $k_r' = 5.2 \times 10^8 \text{ s}^{-1}$ , in water at 23 °C,  $E_r = 4.9 \pm 0.1 \text{ kcal mol}^{-1}$  and  $E_r' = 5.2 \pm 0.3 \text{ kcal mol}^{-1}$ ), and the electron-transfer rate constant ( $k_{ET} = 2.0 \times 10^9 \text{ s}^{-1}$ , in water at 23 °C,  $E_{ET} = 1.8 \pm 0.2 \text{ kcal mol}^{-1}$ ). Solvent viscosity controls the interconversion rate constants while solvent polarity and hydrogen-bonding ability determines the Gibbs energy of electron transfer and the magnitude of its rate constant. Consequently, the nature of tyrosine decays in proteins is determined from a delicate balance between the interconversion and electron-transfer rate constants.

## Introduction

*N*-Acetyltyrosinamide (NAYA) is broadly accepted as an appropriate model compound of a nonterminal tyrosine within a protein.<sup>1–3</sup> The fluorescence lifetime and quantum yield of NAYA are highly sensitive to the presence of water and quenching by amino acids.<sup>1</sup> Hence, the fluorescence decay of a tyrosine residue within a protein reflects the environment of that specific tyrosine. If each tyrosine residue could be described with one single lifetime, the multi-exponential decay of a multityrosine protein would distinguish tyrosines located in different regions of the protein, thus bringing insight into events taking place in these regions of the protein. In this case, time-resolved fluorescence of tyrosines would be a powerful tool to probe protein conformational changes, such as folding, in different zones of the protein.

Unfortunately, the fluorescence decay of a single tyrosine can be intrinsically complex, as shown by the fact that fluorescence decays of NAYA and its analogues within oligopep-

## CHART 1: Molecular Structure of NAYA



ptides, in water at room temperature, can only be fitted with sums of two exponentials.<sup>4–6</sup> In addition, multiple-exponential decays of a single tyrosine protein can also arise from ground-state heterogeneity of the tyrosine interactions with nearby amino acids<sup>4,7</sup> and from dynamic processes in the excited state, which include proton transfer, electron transfer,<sup>8</sup> or energy transfer.<sup>1,2</sup> Consequently, the application of time-resolved fluorescence of tyrosines to the study of structural or conformational changes in proteins has been hampered. Any attempt of obtaining hard structural information from fluorescence, as a result of these different competitive quenching processes, requires unraveling the actual mechanisms and the contribution of each of these processes in the appearance of multiple-exponential decays.

Laws et al.<sup>4</sup> showed that the double-exponential decays of tyrosine (at pH values below 2) and some of its analogues must be due to a process that does not involve photoinduced proton

\* Author to whom correspondence may be addressed. E-mail: macanita@ist.utl.pt.

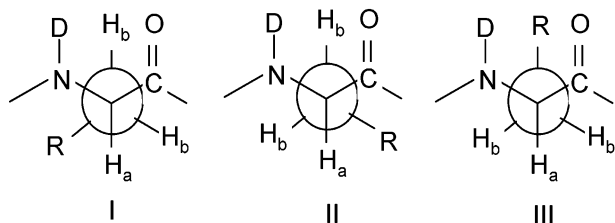
<sup>†</sup> Instituto de Tecnologia Química e Biológica, Universidade Nova de Lisboa.

<sup>‡</sup> REQUIMTE/CQFB, Universidade Nova de Lisboa.

<sup>§</sup> Universidade Técnica de Lisboa.

transfer. They attributed the double exponentiality of NAYA in water to fluorescence heterogeneity of the three rotamers of NAYA, described in terms of the position of the phenol ring in relation to the oligopeptide about the  $C_\alpha-C_\beta$  bond (Chart 2).

**CHART 2: Newman Projections of the Three Principal Rotamers I, II, and III of the Phenol Group in Relation to the  $C_\alpha$  Substituents in NAYA and Analogues as Defined by Laws et al.<sup>4</sup>**



Specifically, rotamer  $C_{II}$ , in which the  $\alpha$ -carbonyl group of the peptide backbone is in close proximity to the phenol ring, has been implicated in a quenching process due to intramolecular electron transfer to the carbonyl group as earlier proposed.<sup>1</sup> Thus, the two exponential terms in the decays of NAYA in water were assigned to the quenched ( $C_{II}$ ) and unquenched ( $C_I$  and  $C_{III}$ ) rotamers of NAYA, and the two pre-exponential coefficients were identified with the ground-state populations of the quenched (short decay time) and unquenched (long decay time) rotamers.

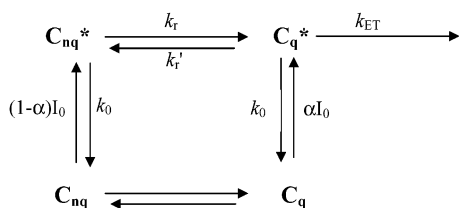
However, Laws' model has certain drawbacks. First, it assumes that the rate of interconversion between the quenched and unquenched rotamers is slow as compared to the de-excitation of individual excited-state rotamers. Second, comparison of the pre-exponential coefficient of the short decay with the population of the quenched rotamer  $C_{II}$ , evaluated by Laws et al.<sup>4</sup> from  $^1H$  NMR spectroscopy showed reasonable agreement for some of the analogues but disagreement for NAYA. Finally, the model fails to explain for transitions from double-exponential to single-exponential decays, which can be experimentally observed with NAYA (see below).

In this work, we will show that the previously described drawbacks result from the assumption that the rate of interconversion between the quenched and unquenched rotamers is slow as compared to the depopulation of individual excited-state rotamers. We will also demonstrate that observation of double-exponential decays with NAYA is exceptional and restricted to narrow ranges of solvent polarity and viscosity, which in turn determine the electron-transfer and the interconversion rate constants, respectively.

**Kinetic Model**

Scheme 1 shows a generalized mechanism for the fluorescence quenching of NAYA, where no assumptions are a priori made on the rates of interconversion between the quenched and unquenched rotamers.

**SCHEME 1**



In this Scheme,  $C_{nq}$  represents the two mutually equivalent ground-state rotamers that are unsusceptible to fluorescence

quenching by electron transfer ( $C_I$  and  $C_{III}$  in Chart 2), and  $C_q$  represents the rotamer where the  $\alpha$ -carbonyl group is placed in close proximity to the phenol ring, thus allowing photoinduced electron transfer (the  $C_{II}$  rotamer in Chart 2).  $C_{nq}$  and  $C_q$  are exchangeable, and their rates of exchange are determined by the rotational rate constants  $k_r$  and  $k_r'$ . In the excited state, the phenol ring of the  $C_q^*$  conformation can transfer an electron to the oligopeptide at a rate constant defined as  $k_{ET}$ . Both rotamers can also decay to the ground state with the rate constant  $k_0 = 1/\tau_0$ , where  $\tau_0$  is the fluorescence lifetime in the absence of any electron transfer. The  $C_q$  population is represented by the molar fraction  $\alpha$ .

**General Solution.** The time evolution of concentrations of the quenched,  $C_q^*$ , and unquenched,  $C_{nq}^*$ , rotamers obey eq 1, where  $X$  and  $Y$  represent the sum of all processes responsible for the deactivation of  $C_{nq}$  and  $C_q$ , respectively (eqs 2 and 3)

$$\frac{d}{dt} \begin{bmatrix} C_{nq}^* \\ C_q^* \end{bmatrix} = \begin{bmatrix} -X & k_r' \\ k_r & -Y \end{bmatrix} \times \begin{bmatrix} C_{nq}^* \\ C_q^* \end{bmatrix} \quad (1)$$

$$X = k_0 + k_r \quad (2)$$

$$Y = k_0 + k_r' + k_{CT} \quad (3)$$

The fluorescence decays of  $C_{nq}$  and  $C_q$  are predicted to be sums of two exponentials as described by eqs 4 and 5, where the reciprocals of the shorter ( $\lambda_2 = 1/\tau_2$ ) and longer ( $\lambda_1 = 1/\tau_1$ ) decay times are related to the rate constants in Scheme 1 by eq 6

$$I_{C_{nq}}(t) = a_{11} e^{-\lambda_1 t} + a_{12} e^{-\lambda_2 t} \quad (4)$$

$$I_{C_q}(t) = a_{21} e^{-\lambda_1 t} + a_{22} e^{-\lambda_2 t} \quad (5)$$

$$\lambda_{2,1} = \frac{X + Y \pm ((X - Y)^2 + 4k_r k_r')^{1/2}}{2} \quad (6)$$

With the initial ( $t = 0$ ) conditions

$$a_{11} + a_{12} = 1 - \alpha \quad (7)$$

$$a_{21} + a_{22} = \alpha \quad (8)$$

the pre-exponentials  $a_{11}$ ,  $a_{12}$ ,  $a_{21}$ , and  $a_{22}$  are expressed as functions of the rate constants  $k_0$ ,  $k_r$ ,  $k_r'$ , and  $k_{ET}$  and the ground-state molar fraction  $\alpha$  of the quenched conformer  $C_q$  by eqs 9–12

$$a_{11} = \frac{(1 - \alpha)(X - \lambda_2) - \alpha k_r'}{\lambda_1 - \lambda_2} \quad (9)$$

$$a_{12} = \frac{\alpha k_r' - (1 - \alpha)(X - \lambda_1)}{\lambda_1 - \lambda_2} \quad (10)$$

$$a_{21} = \frac{(1 - \alpha)(X - \lambda_2) - \alpha k_r'}{k_r'(\lambda_1 - \lambda_2)}(X - \lambda_1) \quad (11)$$

$$a_{22} = \frac{\alpha k_r' - (1 - \alpha)(X - \lambda_1)}{k_r'(\lambda_1 - \lambda_2)}(X - \lambda_2) \quad (12)$$

When both conformers  $C_{nq}$  and  $C_q$  have identical radiative rate constants and identical fractions of emitted light at the

measurement's emission wavelength, the experimentally observed pre-exponential coefficients  $A_1$  and  $A_2$  are the sums of the individual pre-exponentials of the  $C_{\text{nq}}$  and  $C_{\text{q}}$  fluorescence decays (eqs 13 and 14) and are related to the kinetic constant by eqs 15 and 16

$$A_1 = a_{11} + a_{21} \quad (13)$$

$$A_2 = a_{12} + a_{22} \quad (14)$$

$$A_1 = \frac{(1 - \alpha)(X - \lambda_2 - k_r) - \alpha(X - \lambda_1 + k_r')}{\lambda_1 - \lambda_2} \quad (15)$$

$$A_2 = \frac{\alpha(X - \lambda_2 + k_r') - (1 - \alpha)(X - \lambda_1 - k_r)}{\lambda_1 - \lambda_2} \quad (16)$$

**Special Cases.** Let us first consider the following limit conditions: the *slow-exchange limit* where the exchange rates  $k_r$  and  $k_r'$  are much slower than the deactivation rates ( $k_r, k_r' \ll k_0, k_{\text{ET}}$ ) and the *fast-exchange limit* where the excited-state rotamers are in equilibrium ( $k_r, k_r' \gg k_0, k_{\text{ET}}$ ).

In the *slow-exchange limit*,  $X = k_0$  and  $Y = k_0 + k_{\text{ET}}$  (from eqs 2 and 3). Substitution in eqs 6, 15, and 16 leads to the result  $\lambda_1 = k_0, \lambda_2 = k_0 + k_{\text{ET}}, A_1 = 1 - \alpha$ , and  $A_2 = \alpha$ , which predicts double-exponential decays, with decay times equal to the (unquenched and quenched) lifetimes of the rotamers and pre-exponential coefficients  $A_i$  equal to the ground-state populations (molar fractions) of the rotamers. In the (more realistic) special case of slow exchange, defined by  $k_r, k_r', k_0 \ll k_{\text{ET}}$ , the pre-exponential coefficients are still equal to the ground-state populations, but  $\lambda_1 = k_0 + k_r$ , and  $\lambda_2 = k_0 + k_r' + k_{\text{ET}}$ . Hence, both cases of slow exchange are equivalent to Laws' model concerning the physical meaning of the pre-exponential coefficients, although the decay times have different meanings.

In the *fast-exchange limit*,  $X = k_r$  and  $Y = k_r'$ , one obtains  $\lambda_2 = k_r + k_r', \lambda_1 = 0, A_1 = 1$ , and  $A_2 = 0$ , i.e., a single-exponential decay with infinite lifetime. The infinite lifetime ( $\lambda_1 = 0$ ) of course arises from the  $k_0$  and  $k_{\text{ET}} = 0$  approximation. When  $k_0$  and  $k_{\text{ET}} \neq 0$ ,  $\lambda_1$  is approximately equal to the reciprocal weighted average of the rotamers' lifetimes, where the weighting factors are the interchange rate constants  $k_r$  and  $k_r'$  (eq 17)

$$\lambda_1 = \frac{k_r(k_0 + k_{\text{ET}}) + k_r'k_0}{k_r + k_r'} \quad (17)$$

Under the special conditions of  $k_r \gg k_r'$  or  $k_r \ll k_r'$ , eq 17 predicts decay times equal to the lifetime of the quenched ( $k_0 + k_{\text{ET}}$ )<sup>-1</sup> or the unquenched rotamer  $k_0^{-1}$ , respectively, and in the more realistic condition of  $k_r = k_r'$

$$\lambda_1 = k_0 + \frac{k_{\text{ET}}}{2} \quad (18)$$

In all three cases,  $\lambda_1 = k_0$  if  $k_r, k_r', k_0 \gg k_{\text{ET}}$ .

Summarizing, the model predicts for the general case double-exponential decays, where both decay times and pre-exponential coefficients are functions of all rate constants and ground-state populations. In the slow-exchange limit, double-exponential decays, with pre-exponential coefficients equal to the ground-state populations, are still predicted. Finally, for the fast-exchange limit, a single-exponential decay, with a decay time

ranging between the lifetimes of the quenched and the unquenched rotamers, is expected.

## Experimental Section

NAYA was purchased from Sigma and used as such, after verification of purity by HPLC. All other chemicals used were of *spectroscopic* grade with the exception of trifluorethanol and methanol, which were of chromatographic grade and obtained from Aldrich and Merck, respectively. 1,4-Dioxane (Riedel-deHaen) was distilled over sodium in order to remove excess water and a residual impurity; ethanol (Riedel-deHaen), acetonitrile (Merck), and DMSO (Fluka) were used as purchased. *N*-Acetyltyrosine-*N'*-methylamide was synthesized and purified as described in Applewhite and Niemann.<sup>9</sup>

UV-absorption spectra were measured using an Olis-15 double-beam spectrophotometer with 1.0-nm resolution. Steady-state fluorescence excitation and emission spectra were measured using a SPEX Fluorog 2121 spectrofluorimeter. All spectra were collected in the S/R mode and corrected for optics, detector wavelength dependence (emission spectra), and lamp intensity wavelength dependence (excitation spectra). Fluorescence was collected in right angle geometry. Fluorescence quantum yields of NAYA in dioxane water mixtures were determined by comparison to a standard solution of *p*-terphenyl in cyclohexane ( $\phi_f = 0.77$  at 20 °C).<sup>10</sup>

Time-resolved fluorescence measurements were carried out using the single photon counting technique as previously described.<sup>11</sup> Excitation of samples was carried out with the frequency-tripled output of an actively mode-locked picosecond Ti-Sapphire laser (Spectra Physics Tsunami), pumped by a solid-state laser (Spectra Physics Millennia Xs). The repetition rate was set to 4 MHz by passage through an optical-acoustic modulator (Pulse Selector 3980 Spectra Physics). Excitation was vertically polarized and emission was collected at the magic angle of 54.7°. Inverted START-STOP configuration was used in the acquisition. The experimental instrumental response function for all excitation wavelengths was in the 38–42-ps range. Alternate collection of pulse profile and sample decays was performed ( $10^3$  counts at the maximum per cycle) until about  $5 \times 10^3$ – $10^4$  detected counts at the maximum of the fluorescence signal. The fluorescence decays were deconvoluted in a PC, using George Striker's program<sup>12</sup> (LINUX version).

**NMR Spectroscopy and Calculation of Rotamer Populations.** Each NMR sample of a final concentration of 0.2 mg/mL was prepared by dissolving pre-exchanged lyophilized NAYA in 500  $\mu\text{L}$  of deuterated dioxane- $\text{D}_2\text{O}$  at 0, 10, 20, 40, 70, 80, 90, and 100% (v/v) concentration. <sup>1</sup>H NMR spectra of NAYA in  $\text{D}_2\text{O}$  as a function of temperature was measured on a Bruker AMX300 spectrometer at 300.14 MHz. Transients per spectra (48) were acquired with water presaturation during the relaxation delay and using a spectral width of 4.5 kHz and a pulse width of 9  $\mu\text{s}$ . <sup>1</sup>H NMR spectra in deuterated dioxane- $\text{D}_2\text{O}$  mixtures were recorded on a Bruker DRX500 spectrometer operating at 500.18 MHz. A hard pulse of 7  $\mu\text{s}$  covering a 6-kHz sweep was used to collect 48 transients per spectra. Residual solvent suppression was accomplished by applying a pulse train of alternating 25-ms pulses at the observed frequencies of both solvents for a total period of 1 s, immediately followed by the excitation pulse. In all cases, the FID was multiplied by a Gaussian function with a line broadening of -1 Hz and a Gaussian broadening of 0.05, prior to Fourier transform.

The fractional population of rotamers  $C_{\text{q}}$  ( $C_{\text{II}}$ ) and  $C_{\text{nq}}$  ( $C_{\text{I}}$  and  $C_{\text{III}}$ ) was calculated as described previously elsewhere.<sup>4</sup> The fractional population is calculated from the coupling constants between  $\text{H}^\alpha$  and  $\text{H}^{\beta\text{R}}$  ( $\text{H}^{\beta\text{S}}$ ) by applying the following equations

$$p_I = [{}^3J(H^\alpha - H^{\beta R}) - {}^3J_g]/\Delta^3J \quad (19)$$

$$p_{II} = [{}^3J(H^\alpha - H^{\beta S}) - {}^3J_g]/\Delta^3J \quad (20)$$

$$p_{III} = 1 - p_I - p_{II} \\ [{}^3J_t + {}^3J_g - [{}^3J(H^\alpha - H^{\beta R}) + {}^3J(H^\alpha - H^{\beta S})]]/\Delta^3J \quad (21)$$

where  $\Delta^3J = {}^3J_t - {}^3J_g$ ,  ${}^3J_t = 13.56$  Hz, and  ${}^3J_g = 2.6$  Hz are the nominal values of coupling constants for the protons in *trans* and *gauche* conformations, respectively.

**Semiempirical Calculations.** Theoretical calculations were carried out on a personal computer using the HyperChem 5.0 software of Hypercube. Molecular geometries were first optimized using the MM<sup>+</sup> method and refined using the semiempirical AM1 method at the UHF level. Enthalpies of formation and atomic point charges were obtained from single-point AM1 calculations on the optimized geometries.

## Results

**Absorption and Fluorescence Spectra in Dioxane–Water Mixtures.** Dioxane–water mixtures have been widely used in mimicking the microenvironment of fluorescent molecules in heterogeneous media as micelles<sup>13</sup> or microemulsions.<sup>14</sup> In such media, a probe may feel a large span of water content and polarity, which is dictated by its location in the organize. Absorption spectra of NAYA in dioxane–water mixtures show a reduction in the molar extinction coefficient (28.9%), a blueshift of 4 nm, and loss in vibrational structure from pure dioxane to water (Figure 1a). The solvatochromism of NAYA has been explained by a combined effect of dielectric constant ( $\epsilon$ ), the hydrogen-bond donor strength ( $\alpha$ ), and the hydrogen-bond acceptor strength ( $\beta$ ) of the solvent.<sup>15</sup> High dielectric constants and greater  $\alpha$  values tend to displace the spectrum toward the blue, whereas low dielectric constants and greater  $\beta$  values shift the spectrum toward the red (see Discussion for more details).

Fluorescence spectra of NAYA in dioxane–water mixtures undergo a small red shift of 2 nm, from 303 nm in dioxane to 305 nm in water (Figure 1b). However, addition of water quenches the fluorescence of NAYA. The fluorescence quantum yield gradually decreases from 0.17 in pure dioxane to 0.07 in water at 23 °C. The quantum yields in all dioxane–water mixtures also decrease with the increase of temperature (Figure 2).

**Fluorescence Decays in Dioxane–Water Mixtures.** Fluorescence decays of NAYA in dioxane are single exponentials from 23–80 °C, irrespective of excitation and emission wavelengths (Figure 3a). Single-exponential decays are also observed for NAYA in a number of other polar, protic and nonprotic, solvents, at 23 °C (Table 1).

In dioxane–water mixtures (pH  $\approx$  6.5), at 23 °C, the decays can still be fitted with single-exponential functions up to a 70% v/v water content, with lifetimes decreasing from 5.0 ns in dioxane to 3.2 ns in the 40:60 dioxane–water mixture (Figure 4a).

Above 70% water, the decays can only be fitted with sums of two exponentials (Figure 3b). The new short decay time  $\tau_2$  decreases and the respective weight (normalized pre-exponential coefficient  $A_2$ ) increases with water concentration to values of  $\tau_2 = 520$  ps and  $A_2 = 0.12$  in pure water, at 23 °C (Figure 4b). The long decay time ( $\tau_1$ ) further decreases down to a value of 1.57 ns in water, at 23 °C. These observations indicate the existence of at least two species in the excited state, above 70% water.

In contrast with NAYA, the parent compound tyrosine displays single-exponential decays in all dioxane–water mixtures (pH  $\approx$  6.5), with decay times always longer than the longest

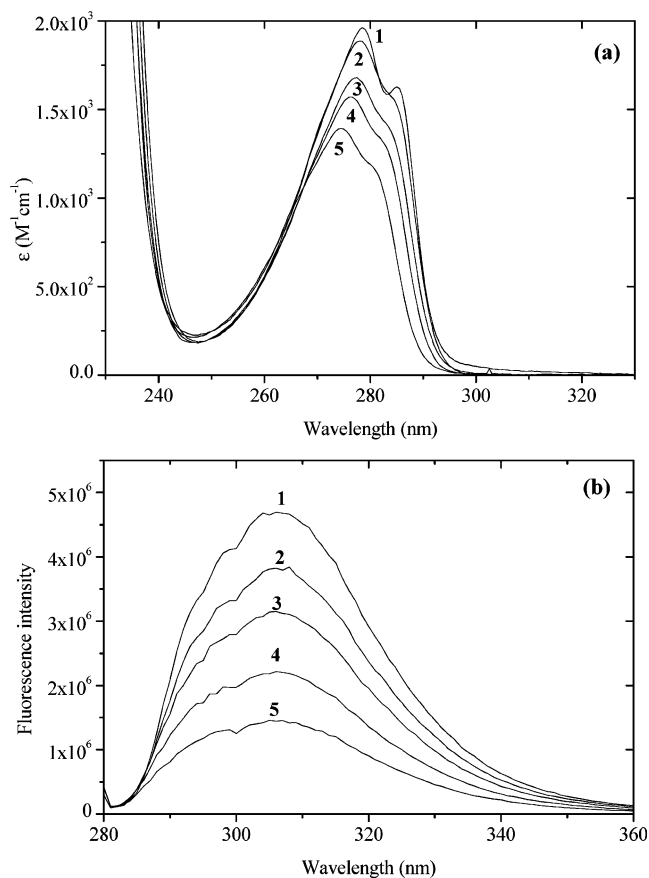


**Figure 1.** Absorption and emission spectra of NAYA in dioxane–water mixtures at 0% (1), 20% (2), 40% (3), 60% (4), and 100% (5) (v/v) water concentration. (a) In the absorption spectra, a blueshift of 4 nm is observed from 278.5 nm at 0% water concentration to 274.5 nm in pure water and a 28.9% decrease in the molar extinction coefficient from  $1962 \text{ dm}^3 \text{ mol}^{-1} \text{ cm}^{-1}$  in dioxane to  $1394 \text{ dm}^3 \text{ mol}^{-1} \text{ cm}^{-1}$  in water. (b) Emission spectra of NAYA in dioxane–water mixtures show a slight redshift of 2 nm from 0 to 100% water and a gradual decrease in the fluorescence quantum yield from 0.17 in 0% water to 0.07 in pure water.

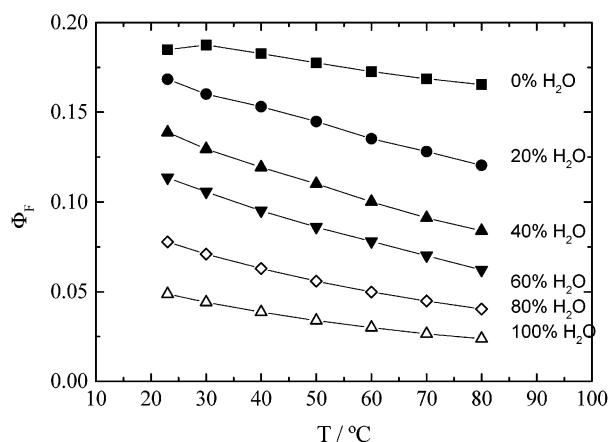


**Figure 2.** Fluorescence quantum yield profiles of NAYA in dioxane–water mixtures.

decay time ( $\tau_1$ ) of NAYA except in the case of dioxane, where the decay times are identical (Figure 4a). Since the chromophores of NAYA and tyrosine are identical, the result shows that water has an *indirect* role in the fluorescence quenching mechanism of NAYA. This result is compatible with the previously proposed intramolecular electron-transfer mechanism.<sup>1,4,8,16</sup>

The existence of double-exponential decays of NAYA was investigated for solvents other than water and observed only in

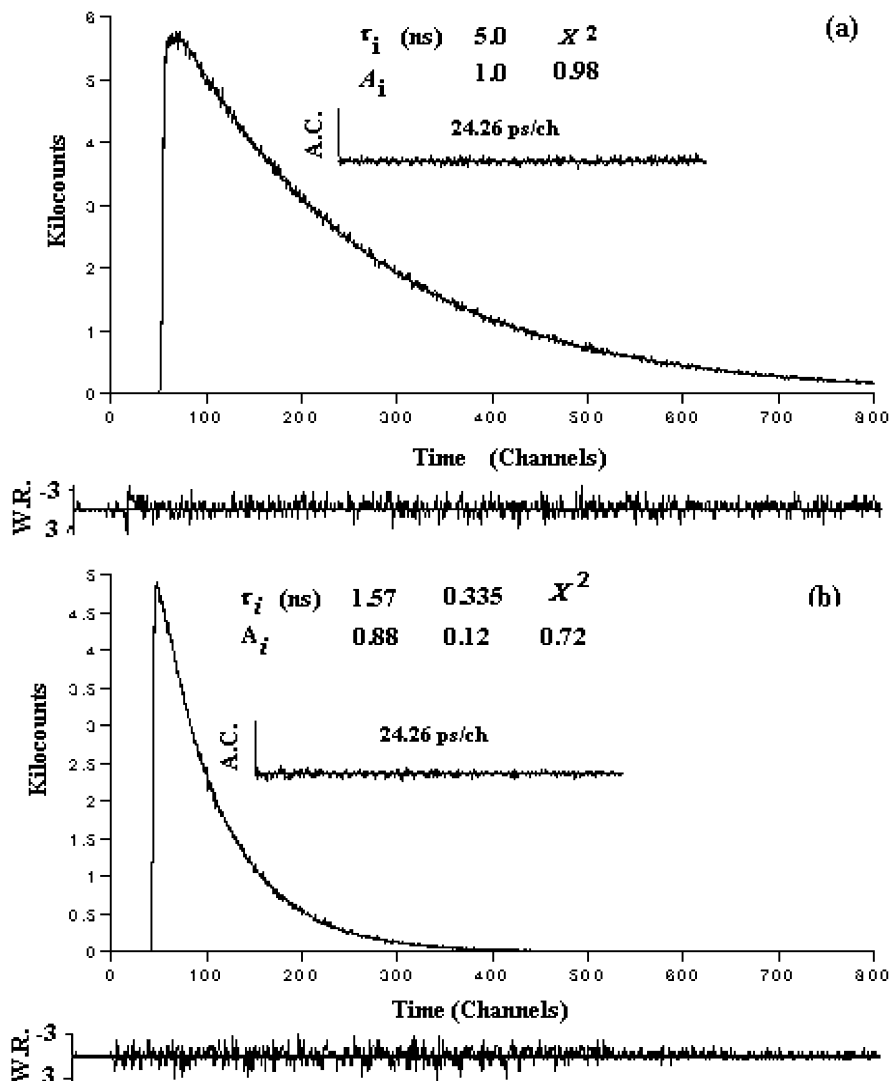


**Figure 3.** (a) Fluorescence decay of NAYA in dioxane at 23 °C with  $\lambda_{\text{ext}} = 287$  nm,  $\lambda_{\text{em}} = 304$  nm, and fit to a single-exponential function with lifetime equal to 5 ns. (b) Fluorescence decay of NAYA in water at 23 °C with  $\lambda_{\text{ext}} = 287$  nm and  $\lambda_{\text{em}} = 305$  nm is double exponential with decay times of 1.57 and 0.33 ns and pre-exponential coefficients of 0.88 and 0.12, respectively. Autocorrelation functions, weighted residuals, and  $\chi^2$  values are also shown.

**TABLE 1: Maximum Absorption ( $\lambda_{\text{abs}}$ ) and Emission ( $\lambda_{\text{em}}$ ) Wavelengths, Fluorescence Decay Times ( $\tau_1$  and  $\tau_2$ ), and Normalized Pre-Exponential Coefficients ( $A_1$  and  $A_2$ ) of NAYA as a Function of Solvent Dielectric Constant ( $\epsilon$ ) and Kamlet–Taft Parameters ( $\alpha$ ,  $\beta$ , and  $\pi^*$ )<sup>a</sup>**

solvent	$\epsilon$	$\alpha$	$\beta$	$\pi^*$	$\lambda_{\text{abs}}$ (nm)	$\lambda_{\text{em}}$ (nm)	$\tau_1$ (ns)	$\tau_2$ (ns)	$A_1$	$A_2$
dioxane	2.2	0	0.37	0.55	278.5	303	4.95		1.00	
DMSO	48	0	0.76	1.0	280	307	1.51		1.00	
acetonitrile	37.5	0.19	0.31	0.6	277	304	4.35		1.00	
ethanol	24.3	0.83	0.77	0.54	278	306	3.64		1.00	
methanol	32.6	0.93	0.62	0.60	277	305	3.52		1.00	
water	78.5	1.17	0.40	1.09	274.5	305	1.57	0.34	0.88	0.12
trifluoroethanol	26	1.51	0	0.73	273.5	305	1.49	0.48	0.81	0.19

<sup>a</sup> Only in water and trifluoroethanol are double-exponential fits required ( $A_2 \neq 0$ ).

the case of the strong hydrogen-bond donor solvent trifluoroethanol (Table 1). In water, decay measurements were also carried out as a function of pH (2.5–8) and emission wavelength (290–360 nm), and no changes were observed in decay times or pre-exponential coefficients (Figure 5) along the emission band or upon changes in pH. The observed independence of pH excludes excited-state proton transfer phenomena as the origin of the double-exponential decays of NAYA in water. Not the least important, independence of emission wavelength shows that the two decay times have exactly the same spectral

distribution (emission spectrum). These observations are also compatible with the “rotamers’ model”.

Fluorescence decays of NAYA in water were also independent of concentration of NAYA (0.214–1.72 mM) and excitation wavelength (260, 275, and 287 nm), thus excluding aggregation and complex formation as the origin of the double-exponentiality of NAYA in water.

**Fluorescence Decays in Water as a Function of Temperature.** The increase of temperature induces a general decrease of both decay times of NAYA in water (Figure 6a) and a decrease

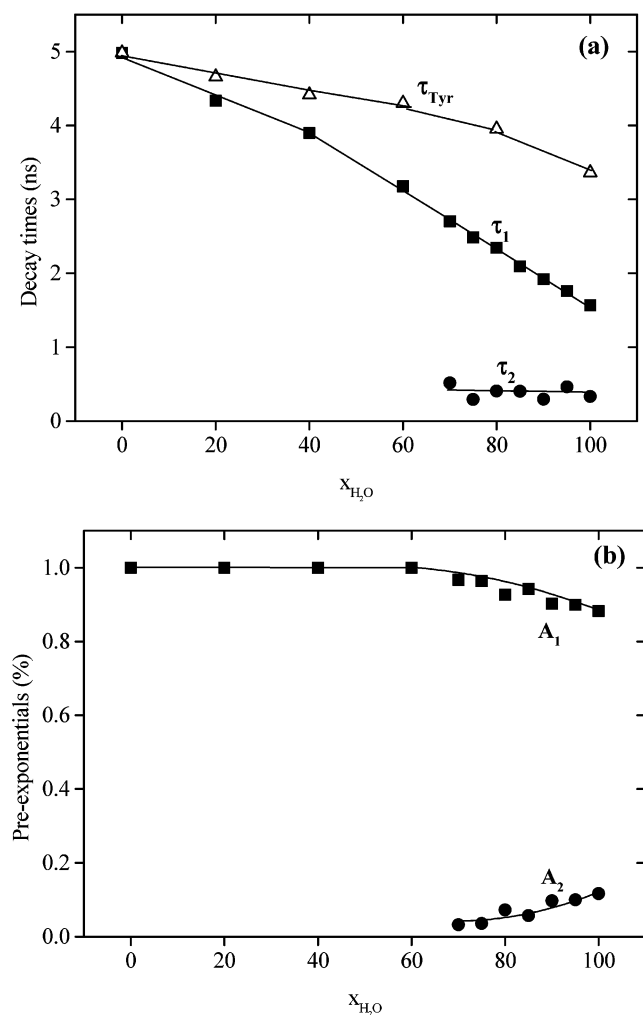


**Figure 4.** (a) Fluorescence decay times of NAYA,  $\tau_1$  (■),  $\tau_2$  (●), and tyrosine ( $\Delta$ ) in dioxane–water mixtures. Below 70% v/v water concentration, decays of NAYA are single exponentials and the lifetime in dioxane is equal to the lifetime of tyrosine. (b) Normalized pre-exponential coefficients.

in the pre-exponential coefficient  $A_2$  of the shorter decay time  $\tau_2$  (Figure 6b). Significantly, above 50 °C,  $A_2$  becomes so close to zero that the decays can be fitted with single exponentials.

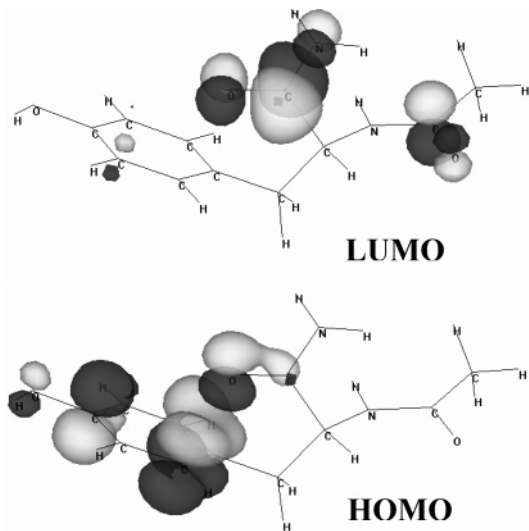
The foregoing results show that observation of double-exponential decays with NAYA is an exception, not the rule, critically depending on solvent and temperature. This is contrary to the widespread belief<sup>2,4</sup> that NAYA generally decays as a double-exponential function.

**NMR Results.** The coupling constants ( $^3J(\text{H}^\alpha\text{--H}^{\beta R})$  and  $^3J(\text{H}^\alpha\text{--H}^{\beta S})$ ) of NAYA in  $\text{D}_2\text{O}$  were measured as a function of temperature and are presented in Table 2. The coupling constants show a constant profile within experimental error with increasing temperature, and as a result, the fractional population of the quenched conformation ( $\alpha$ ) is fairly constant in the temperature range from 20 to 80 °C.

The coupling constant  $^3J(\text{H}^\alpha\text{--H}^{\beta S})$  associated to the population of the quenched conformation ( $\alpha$ ) was also measured in deuterated dioxane– $\text{D}_2\text{O}$  mixtures, at 27 °C. In this case, a significant although small variation of  $\alpha$  was observed (Table 2). Interestingly, this variation seems to be inversely proportional to the viscosity of the deuterated dioxane– $\text{D}_2\text{O}$  mixtures (Figure 7).

**Theoretical Results.** In Chart 3, sketches of the HOMO and the LUMO of model compound NAYA, obtained with AM1

**CHART 3: Sketches of Electron Density of the HOMO and LUMO of Model Compound NAYA Calculated by AM1**



geometry optimization and single-point calculations, is depicted. Chart 3 shows that, in the quenched rotamer  $\text{C}_q$ , the phenol and the amide carbonyl groups are in close contact and that the HOMO has its highest probability density on the chromophore (cresol) of NAYA, while the LUMO is localized on the amide carbonyl group of the peptide.

The vertical ionization energy of cresol (gas phase) IP was calculated from the AM1 formation enthalpies of cresol  $\Delta_f H^{298}$  (−1.30 eV) and its radical cation (7.03 eV), with a result of IP =  $\Delta\Delta_f H^{298}$  = 8.33 eV, in reasonable agreement with the experimental value of IP = 8.36 eV.<sup>17</sup> The gas-phase electron affinity EA of *N*-acetylglycinamide was similarly calculated from the AM1 formation enthalpies of *N*-acetylglycinamide and its radical anion with the result EA = 0.26 eV. We were not able to find experimental data on the electron affinity of this compound or similar amides.

A crude evaluation of the Gibbs energy of electron transfer from the phenol to the amide moieties in the excited state in water  $\Delta G^\circ$  was carried out using in eq 22 the calculated IP and EA values, the excitation energy of NAYA in water  $h\nu = 4.32$  eV, the Coulombic interaction of the products (radical ions) in water,  $\Delta G_{\text{ionic}} = -0.03$  eV (eq 23), and the correction of IP and EA for solvation of the ion radicals in water  $\Delta\Delta G_{\text{solv}} = -4.44$  eV (eq 24<sup>18</sup>)

$$\Delta G^\circ = \text{IP} - \text{EA} - h\nu + \Delta G_{\text{ionic}} + \Delta\Delta G_{\text{solv}} \quad (22)$$

$$\Delta G_{\text{ionic}} = -\frac{e^2}{\epsilon_{\text{solv}}(r_{\text{cresol}} + r_{\text{amide}})} \quad (23)$$

$$\Delta\Delta G_{\text{solv}} = -\frac{e^2}{2}(r_{\text{cresol}}^{-1} + r_{\text{amide}}^{-1})(\epsilon_{\text{solv}}^{-1} - 1) \quad (24)$$

The estimated value of  $\Delta G^\circ = -0.72$  eV indicates that intramolecular electron transfer occurring with NAYA in the excited state and in aqueous solution should be exothermic. This is close to the value of the standard free energy of electron transfer from *p*-cresol to the peptide group in water,  $\Delta G^\circ \leq -0.49$  eV, which has been predicted from electrochemical data in dimethylformamide.<sup>19</sup>

Summarizing all results, three relevant facts emerge. First, we have observed that neither excited-state proton transfer,

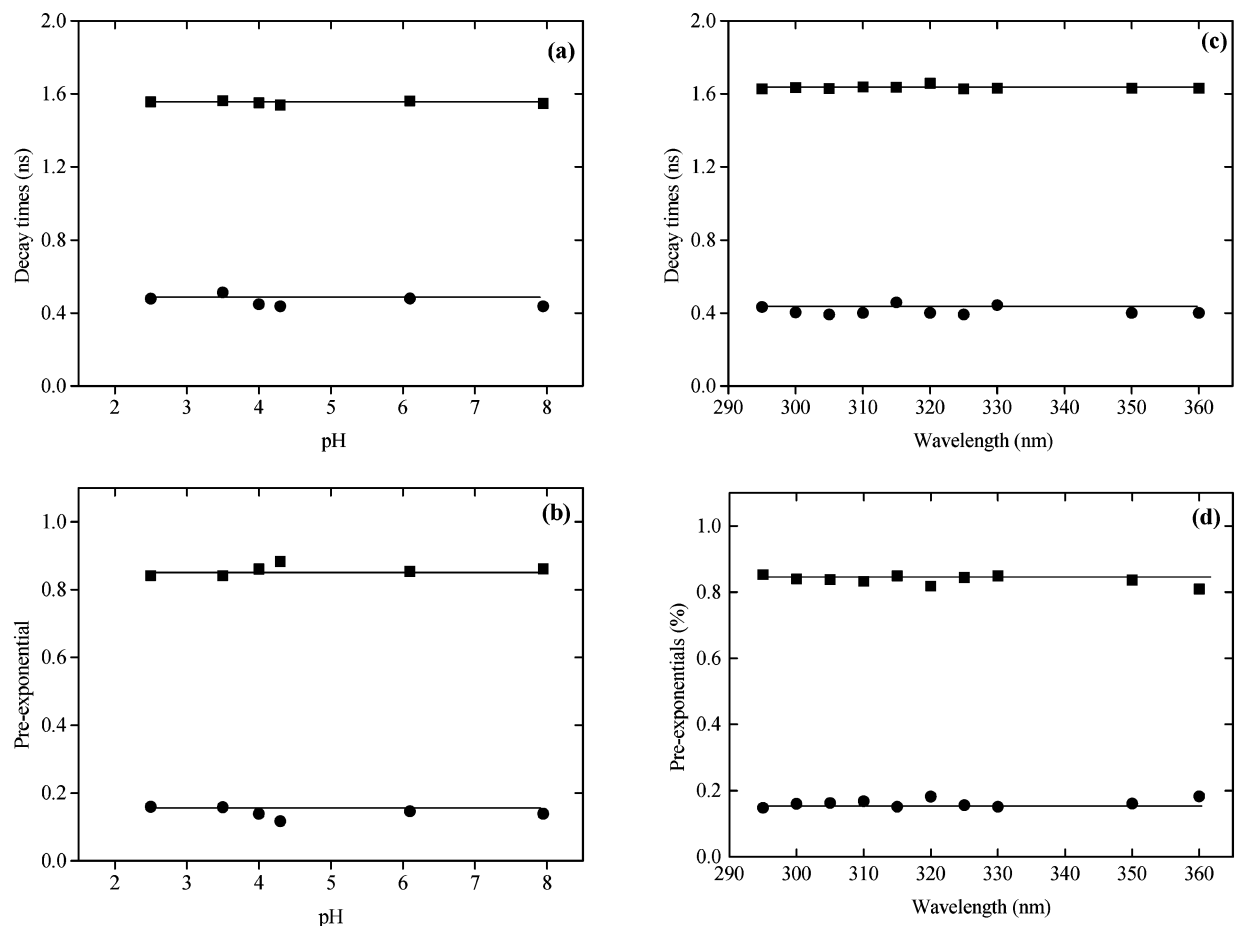


**Figure 5.** (a) Decay times ( $\tau_1$  and  $\tau_2$ ) and (b) pre-exponential coefficient ( $A_1$  and  $A_2$ ) of NAYA measured at 23 °C, pH 6, and excitation wavelength of 275 nm show no change as a function of pH. (c) The decay times and (d) pre-exponential coefficients at pH 6 and  $\lambda_{\text{ext}} = 287$  nm at 23 °C also showed no change as a function of emission wavelength.

**TABLE 2: Values of  $^1\text{H}$  NMR Coupling Constants ( $^3J(\text{H}^\alpha\text{--H}^{\beta\text{S}})$  and  $^3J(\text{H}^\alpha\text{--H}^{\beta\text{R}})$ ) and Calculated Quenched Rotamer Population ( $\alpha$ ) in  $\text{D}_2\text{O}$  as a Function of Temperature and in Deterated Dioxane– $\text{D}_2\text{O}$  Mixtures at 27 °C**

$T$ (°C)	coupling constants (Hz)			$\alpha$	$\text{D}_2\text{O--DX}$	coupling constants (Hz)			$\alpha$
	$^3J(\text{H}^\alpha\text{--H}^{\beta\text{S}})$	$^3J(\text{H}^\alpha\text{--H}^{\beta\text{R}})$				$^3J(\text{H}^\alpha\text{--H}^{\beta\text{S}})$	$^3J(\text{H}^\alpha\text{--H}^{\beta\text{R}})$		
20	6.05	8.75	0.31	0	7.61	6.69	0.46		
30	6.0	8.75	0.31	10	6.78	7.89	0.36		
40	6.18	8.66	0.33	20	6.23	8.16	0.34		
50	6.18	8.86	0.33	40	6.05	8.80	0.31		
60	6.05	8.66	0.31	70	5.55	9.17	0.29		
70	6.05	8.66	0.31	80	5.73	9.03	0.29		
80	6.05	8.73	0.31	90	5.87	9.17	0.30		
				100	6.19	8.89	0.33		

aggregation, or complex formation is implicated as the origin of the double-exponential decays of NAYA in water, in agreement with other authors.<sup>4,8</sup> Second, the two decay times show the same emission spectral distribution, thus supporting the proposed assignment of the two excited-state species to two differently quenched rotamers,<sup>4</sup> while the calculated  $\Delta G^\circ$  value supports electron transfer as an efficient quenching mechanism in water. Finally, observation of double-exponential decays with NAYA, as a result of electron transfer, is restricted to highly polar solvents and to limited temperature ranges. This last fact has obvious implications on the interpretation of fluorescence decays of tyrosine within a protein, where both the polarity and viscosity of the tyrosine's microenvironment can substantially change.

## Discussion

The solvent effect of NAYA can be rationalized on the basis of the fact that the HOMO of NAYA has significant contribution of a *p*-orbital (electron lone pair) of the phenolic oxygen and the LUMO has less. Thus, electronic excitation induces charge transfer from the hydroxyl oxygen to the phenyl group,<sup>20</sup> which has two consequences. First, the dipole moment is reduced in the excited state (from 1.33 D in the ground state to 1.15 D in the excited state, AM1 calculations). A similar decrease of the dipole moment in the excited state was also observed in the case of cresol by Ross and Lee.<sup>15</sup> Second, the phenolic hydroxyl group becomes more acidic<sup>21–23</sup> and a better hydrogen donor in the excited state, while it is essentially a hydrogen-bond acceptor in the ground state. Consequently, the absorption

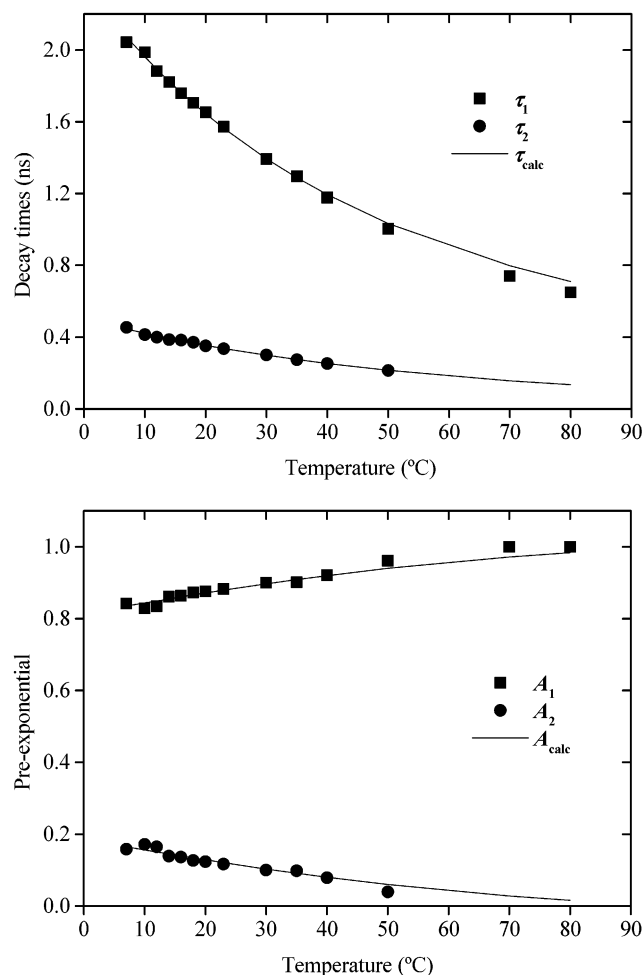


**Figure 6.** (a) Fluorescence decay times of NAYA in pure water, at pH 6,  $\lambda_{\text{ext}} = 275$  nm, and  $\lambda_{\text{em}} = 305$  nm as a function of temperature decrease with increasing temperature. (b) The pre-exponential coefficient of the shortest decay time  $A_2$  decreases with increasing temperature. Above 50 °C, the decays are single-exponential functions. The lines in a and b are calculated values of  $\tau_1$ ,  $\tau_2$ ,  $A_1$ , and  $A_2$  using the kinetic model.

spectrum of NAYA, whose solvent-induced energy change essentially depends on solvation of the ground state, is blue-shifted in solvents of higher dielectric constant (higher Kamlet–Taft  $\pi^*$  values) and higher hydrogen-bond donor strength (higher Kamlet–Taft  $\alpha$  values), such as water and trifluoroethanol (Table 1). On the other hand, the fluorescence spectrum, depending on solvation of the excited state, is redshifted in solvents of lower dielectric constant and higher hydrogen-bond acceptor strength (higher Kamlet–Taft  $\beta$  values), as is in ethanol and DMSO.<sup>15</sup> In this connection, it has been shown in the case of tyrosine that the presence of proton acceptors such as acetate, phosphate, and imidazole slightly shifts the fluorescence spectrum toward the red.<sup>24</sup> Opposing effects of  $\epsilon$  and  $\beta$  on the emission spectrum of NAYA may occur in solvents with high  $\epsilon$  and  $\beta$  values and result in very small solvent-induced shifts as observed from dioxane to water.

The first absorption band of NAYA is due to the symmetry forbidden  $^1L_b$ -like transition of cresol,<sup>15</sup> whose oscillator strength also depends on (and increases with) the contribution of the p orbital (electron lone pair) of the phenolic oxygen in the HOMO and LUMO. This contribution is likely to be lowered in hydrogen-bond donor solvents and increased in hydrogen-bond acceptors. Molecular orbital calculations carried out by Ross and Lee<sup>15</sup> indicated an increase in the oscillator strength up to 26% in the

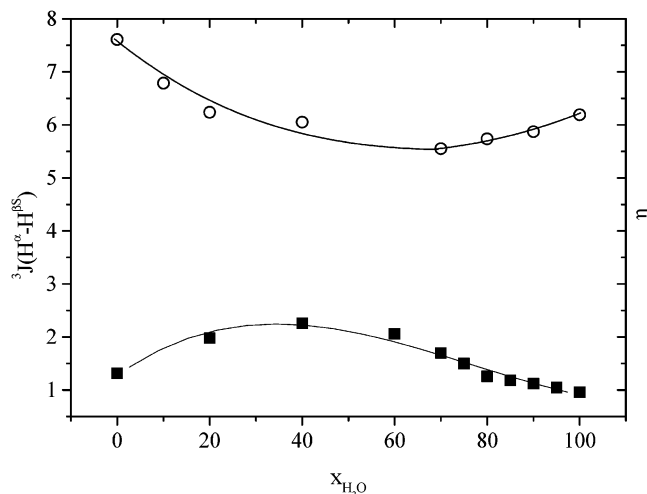


**Figure 7.** Coupling constant (○) associated with the population of the quenched conformation of NAYA measured in deuterated dioxane–D<sub>2</sub>O mixtures at 27 °C shows a decrease from 0 to 40% (v/v) water concentration and an increase from 70 to 100% (v/v) water concentration. This profile is similar to the inverse tendency of viscosity (■) for dioxane–water mixtures.

presence of proton acceptors such as the carbonyl groups of the peptide chain in proteins or carboxyl groups of nearby glutamic or aspartic amino acids. Indeed, the extinction coefficient of NAYA (Table 1) has its lowest and highest values, respectively, in trifluoroethanol ( $\alpha = 1.51$  and  $\beta = 0$ ) and DMSO ( $\alpha = 0$  and  $\beta = 0.76$ ). From dioxane to water, a comparable decrease of the extinction coefficient (29%) is observed (Figure 1a).

**Kinetic Analysis of Fluorescence Data.** In Scheme 1, there are 5 unknowns ( $k_r$ ,  $k_r'$ ,  $k_0$ ,  $k_{\text{ET}}$ , and  $\alpha$ ), but analysis of the decay data (using the kinetic model) provides only three equations ( $\lambda_1$ ,  $\lambda_2$ , and the ratio of the pre-exponential coefficients  $A_2/A_1$ ). The number of unknowns is reduced to three in the following manner.

First,  $k_0$  was measured with tyrosine, as the model compound of the unquenched conformers of NAYA. Tyrosine was chosen because electron transfer to the *ionized* carboxylate group does not occur,<sup>4</sup> therefore showing single-exponential decays and lifetimes longer than those of NAYA in water.<sup>25</sup> Accordingly, in nonpolar solvents such as dioxane, where electron transfer with NAYA does not occur, NAYA and tyrosine show identical lifetimes. Furthermore, the predicted variation of the radiative rate constant of tyrosine from dioxane to water (using the experimental extinction coefficients of NAYA in the Strickler–Berg equation)<sup>26</sup> matches the observed variation of the reciprocal decay time of tyrosine.

Second, the molar fraction of quenched conformers  $\alpha$  was determined using two approaches: (i) directly, by NMR spectroscopy or (ii) by assuming that the rotamers' exchange rates do not change from the ground to the excited state. Under this assumption,  $k_r$  and  $k_r'$  are related to the ground-state population of the quenched conformer  $\alpha$  by eq 25, where the factor 2 in denominator arises from the number of unquenched conformers (two). When  $k_r = k_r'$ , all rotamers are equally probable, i.e.,  $\alpha = 1/3$

$$k_r' = \frac{1 - \alpha}{2\alpha} k_r \quad (25)$$

Finally, since the quenched and unquenched rotamers must have identical emission spectra and radiative constants, each experimental pre-exponential coefficient,  $A_1$  or  $A_2$ , is the sum



**TABLE 3: Ground-State Population of the Quenched Rotamer ( $\alpha$ ), Reciprocal Lifetime of Tyrosine ( $k_0$ ), Rate Constants of Rotamers Exchange ( $k_r$ ,  $k_r'$ ), and Rate Constant of Intramolecular Electron Transfer ( $k_{ET}$ ) of NAYA in Water, at 7, 23, and 50 °C**

rate constant	T/°C			A <sup>a</sup> (ps <sup>-1</sup> )	E <sub>a</sub> <sup>a</sup> (kcal/mol)
	7	23	50		
$\alpha$	0.320	0.300	0.290		
$k_0/\text{ns}^{-1}$	0.254	0.297	0.372	0.0045	$1.60 \pm 3.1 \times 10^{-9}$
$k_r/\text{ns}^{-1}$	0.289	0.442	1.01	$1.8 \pm 0.1$	$4.9 \pm 0.1$
$k_r'/\text{ns}^{-1}$	0.308	0.522	1.25	$3.7 \pm 0.1$	$5.2 \pm 0.3$
$k_{ET}/\text{ns}^{-1}$	1.58	2.06	2.66	$0.11 \pm 0.01$	$1.8 \pm 0.2$

<sup>a</sup> Values of the frequency factor (A) and activation energy ( $E_a$ ) evaluated from Arrhenius plots of the rate constants are also shown.

of the pre-exponential coefficients of both rotamers (eqs 13 and 14) and is given by eqs 15 or 16, respectively.

Evaluation of the four unknowns ( $k_r$ ,  $k_r'$ ,  $k_{ET}$ ,  $\alpha$ ) was carried out as follows:  $k_{ET}$  is calculated by substituting eq 2 and the sum of  $\lambda_1$  and  $\lambda_2$  in the ratio of pre-exponential coefficients,  $R = A_2/A_1$ , calculated from eqs 15 and 16 and rearranged to obtain eq 26

$$k_{ET} = \left( \frac{R\lambda_2 + \lambda_1}{R + 1} - k_0 \right) / \alpha \quad (26)$$

When  $\alpha$  is determined by NMR,  $k_{ET}$  is obtained straightforwardly from eq 26.  $k_r$  is determined from eq 30, which is obtained by substituting eqs 27 in 28 and 28 in 29. Equation 27 is the sum of  $\lambda_1$  and  $\lambda_2$  rearranged as a function of  $k_r$  and  $k_r'$ , eq 28 is the product of X and Y, calculated from eqs 2 and 3, and eq 29 is obtained from the difference of  $\lambda_1$  and  $\lambda_2$

$$\lambda_1 + \lambda_2 - 2k_0 - k_{ET} = k_r + k_r' \quad (27)$$

$$XY = k_0^2 + k_0(k_r + k_r') + k_r k_r' + k_0 k_{ET} + k_r k_{ET} \quad (28)$$

$$\lambda_1 \lambda_2 = XY - k_r k_r' \quad (29)$$

$$k_r = \frac{\lambda_1 \lambda_2 - k_0 - k_0(k_r + k_r')}{k_{ET}} - k_0 \quad (30)$$

$k_r'$  is then determined directly from eq 25.

When  $\alpha$  is defined by eq 25, the kinetics can still be solved without using the molar fractions measured with NMR spectroscopy. These in turn serve as an independent verification of the kinetic analysis. In this case, an iterative process is employed where  $k_r$  and  $k_r'$  are first calculated using the same procedure as stated above with an initial guess of  $\alpha$ . When the imposed value of  $\alpha$  is equal to the value determined by eq 25, the iteration process is terminated. Self-consistency was always obtained independently of the initial guess value.

#### Rate Constants in Water as a Function of Temperature.

Values of the rate constants  $k_0$ ,  $k_r$ ,  $k_r'$ , and  $k_{ET}$  and the population of the quenched rotamer  $\alpha$ , in water, at three temperatures, are given in Table 3, and Arrhenius plots of the rate constants are shown in Figure 8.

First, we note that all rate constants have the same order of magnitude; i.e., neither the slow nor the fast-exchange limit applies. Consequently, the pre-exponential coefficients of the decays have no direct physical meaning. On the other hand, the kinetic analysis yields the correct value for the population of the quenched rotamer ( $\alpha = 0.30$  at 23 °C), in agreement with <sup>1</sup>H NMR data ( $\alpha = 0.31$ ) as seen in Table 2. Similarly, the decay times also do not have a direct physical meaning, and cannot be used, alone or combined as the so-called “mean

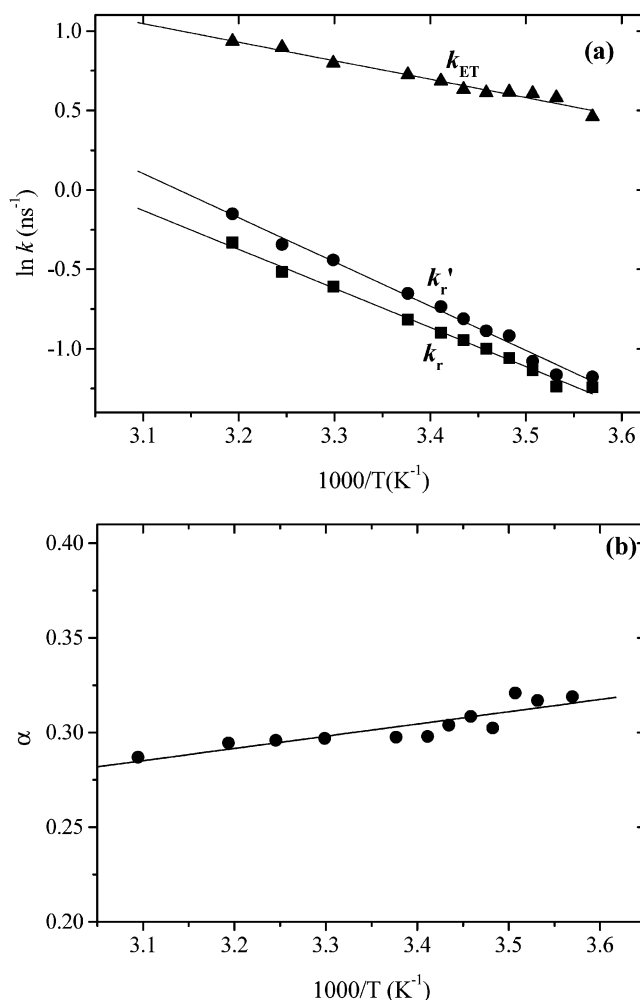


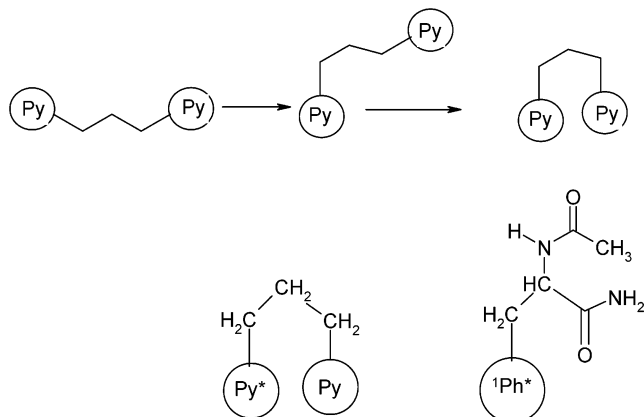
**Figure 8.** (a) Arrhenius plots of rotational rate constants  $k_r$  and  $k_r'$  and electron-transfer rate constant  $k_{ET}$ . (b) Plot of the molar fraction of quenched conformer  $\alpha$  as a function of reciprocal temperature.

lifetime”, in evaluating the electron-transfer rate constant from  $k_{ET} = k_0 - 1/\tau_{\text{mean}}$ .<sup>27</sup> As an example, such procedure when applied to our data at 23 °C gives the value  $k_{ET} = 0.4 \text{ ns}^{-1}$ , while the full kinetic analysis yields a 5-fold larger value ( $k_{ET} = 2.0 \text{ ns}^{-1}$ ).

Second, we observe that the interconversion rate constants  $k_r$  and  $k_r'$  have similar values at 23 °C ( $4.4 \times 10^8$  and  $5.2 \times 10^8 \text{ s}^{-1}$ ) and similar activation energies (4.9 and 5.2 kcal mol<sup>-1</sup>). The lack of information on the order of magnitude of these rotational rates has been a drawback in interpreting the double-exponential decays of NAYA.<sup>4,5,8</sup> However, rotational rate constants can be accessed from end-to-end intramolecular excimer formation data, obtained with molecules with the appropriate chain ends. Specifically, intramolecular excimer formation with 1,3-(1,1'-dipyrenyl) propane, Py(3)Py, involves a transition to the excimer conformation similar to the transition to the quenched rotamer in the case of NAYA (Chart 4). Also in the case of Py(3)Py, the fraction of the rotamer population  $\alpha$  has been measured by <sup>1</sup>H NMR.<sup>28,29</sup>

Although not measured in water, the rate constant of excimer formation with Py(3)Py ( $k_a$ ) was accurately measured in a large number of hydrocarbon solvents as a function of temperature.<sup>30</sup> From these data, the interpolated values of  $k_a$  and  $E_a$  for a solvent viscosity equal to that of water (1 cP at 20 °C) are  $1.15 \times 10^8 \text{ s}^{-1}$  and 4.9 kcal/mol, which agree with the  $k_r$  and  $E_r$  values in Table 3. Therefore, the orders of magnitude of both rate

**CHART 4: Comparison of Conformations in 1,3-(1,1'-Dipyrenyl) Propane (Py\*)-(Py) Which Favor Intramolecular Excimer Formation with the Quenched Rotamer in the Case of NAYA (Chart 3), Where the Phenol Rings Is Placed in Close Proximity to the Carbonyl Peptide Group**



constants  $k_r$  and  $k_r'$  and activation energies  $E_r$  and  $E_r'$  are fully compatible with a solvent-controlled alkane-chain rotation.

Third, the experimental value of electron-transfer activation energy  $E_{ET} = 1.8$  kcal/mol is small as expected from the value of the standard free energy of electron transfer from *p*-cresol to the peptide group,  $\Delta G^\circ \leq -0.49$  eV<sup>19</sup> ( $-11.3$  kcal/mol). This value of  $\Delta G^\circ$  predicts for the activation Gibbs' energy,  $\Delta G^\ddagger$ , a value smaller than 4.4 kcal/mol (using a value  $\lambda = 36.8$  kcal/mol for the repolarization energy and  $\Delta G^0 = -11.3$  kcal/mol in Marcus's relation given by eq 31). The value of the Arrhenius pre-exponential factor  $A = 1.1 \times 10^{11} \text{ s}^{-1}$ , also has the expected order of magnitude<sup>31</sup>

$$\Delta G^\ddagger = \frac{(\Delta G^0 + \lambda)^2}{4\lambda} \quad (31)$$

**Rate Constants in Dioxane–Water Mixtures.** Values of  $k_0$ ,  $k_r$ ,  $k_r'$ , and  $k_{ET}$  in dioxane–water mixtures, at 23 °C, as well as physical data of these mixtures are given in Table 4. The interconversion (rotational) rate constants  $k_r$  and  $k_r'$  should be proportional to the reciprocal viscosity). Log–log plots of  $k_r$  and  $k_r'$  vs viscosity (Figure 9) indeed give values for the slopes equal to  $-1.08 \pm 0.2$  and  $-0.83 \pm 0.1$ , which differ slightly from the expected linear dependence of slopes equal to  $-1$  ( $k = (\text{const})\eta^{-1}$ ) due to the inherent difficulty of determining precisely the correct pre-exponential factor of the smallest

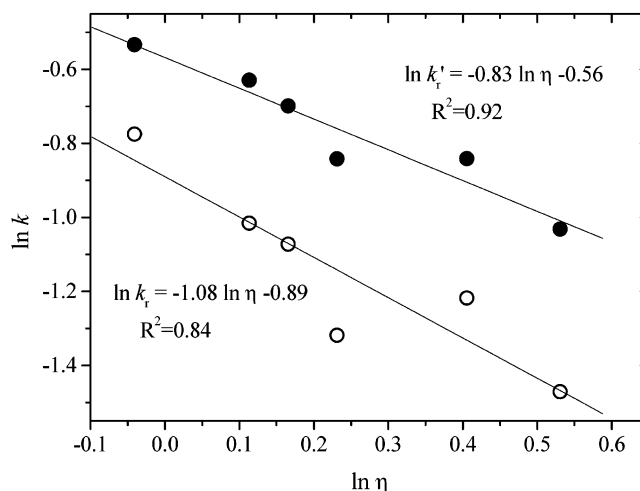


**Figure 9.** Log–log plots of rotational rate constants  $k_r$  and  $k_r'$  vs viscosity  $\eta$  show slopes equal to  $-1.08 \pm 0.2$  and  $-0.83 \pm 0.1$ , respectively.

lifetime ( $\tau_2$ ), which contributes to less than 3% of the total fluorescence intensity.

The electron-transfer rate constant  $k_{ET}$  shows the expected increase with solvent polarity from the 30/70 v/v dioxane–water mixture to neat water. In an attempt to analyze the effect of solvent polarity on  $k_{ET}$ , we evaluated the standard free energy of electron transfer from cresol to the peptide group in the foregoing mixtures, using eq 32<sup>32</sup>

$$\Delta G_{ET}^0 = E_{D/D^+}^0 - E_{N/N^-}^0 - hv + \Delta G(\epsilon) \quad (32)$$

where  $E_{D/D^+}^0 = 1.4$  V is the oxidation potential for cresol in acetonitrile (AN)<sup>19</sup> and  $E_{N/N^-}^0 = -2.85$  V is the reduction potential of NAYA in dimethylformamide (DMF).<sup>19</sup>  $hv$  is the excitation energy taken as the mid energy value of the absorption and emission spectra of NAYA in the dioxane–water mixtures and  $\Delta G(\epsilon)$ , defined in eq 33,<sup>33,34</sup> corrects the reduction and oxidation potentials for (i) the ionic interaction energy of radical ions with a radius  $r_{ion}$  in a complex with a center to center distance  $a_{EC}$  and (ii) the difference in ion solvation, from the reference solvent DMF (or AN) with dielectric constant  $\epsilon_{DMF}$  and the dioxane–water mixture of interest or neat water ( $\epsilon$ )

$$\Delta G(\epsilon) = \frac{e^2}{4\pi\epsilon_0} \left[ \left( \frac{1}{r_{ion}} - \frac{1}{a_{EC}} \right) \frac{1}{\epsilon} - \frac{1}{r_{ion}\epsilon_{DMF}} \right] \quad (33)$$

As pointed out by Seidel et al., using the parameters  $r_{ion} = 3$  Å and  $a_{EC} = 7$  Å, eq 33 fails to predict the experimentally

**TABLE 4: Values of the Reciprocal Lifetime of Tyrosine ( $k_0$ ), Rate Constants of Rotamer Exchange ( $k_r$ ,  $k_r'$ ), Rate Constant of Intramolecular Electron Transfer ( $k_{ET}$ ) of NAYA, and Molar Fraction of the Quenched Rotamer ( $\alpha$ ) as a Function of Dielectric Constant ( $\epsilon$ ) and Viscosity ( $\eta$ ) in Dioxane–Water Mixtures at 23 °C**

dioxane–water mixture v/v % water	$\epsilon$	$\eta^{23 \text{ °C}}$ (cP)	$k_0$ (ns <sup>-1</sup> )	$k_r$ (ns <sup>-1</sup> )	$k_r'$ (ns <sup>-1</sup> )	$k_{ET}$ (ns <sup>-1</sup> )	$\alpha$
0	2.21	1.32	0.201				
20	10.92	1.98	0.215				
40	27.80	2.26	0.227				
60	45.0	2.06	0.233				
70	54.5	1.7	0.240 <sup>a</sup>	0.230	0.356	0.591	0.273
75	58.9 <sup>a</sup>	1.5	0.245 <sup>a</sup>	0.296	0.431	0.659	0.280
80	63	1.26	0.253	0.267	0.430	0.937	0.286
85	67 <sup>a</sup>	1.18	0.260 <sup>a</sup>	0.342	0.497	1.08	0.290
90	72	1.12	0.270 <sup>a</sup>	0.362	0.532	1.44	0.298
95	75 <sup>a</sup>	1.05	0.280 <sup>a</sup>	0.379	0.464	1.74	0.30
100	78.4	0.96	0.297	0.461	0.587	1.98	0.31

<sup>a</sup> Estimated and analytically resolved.

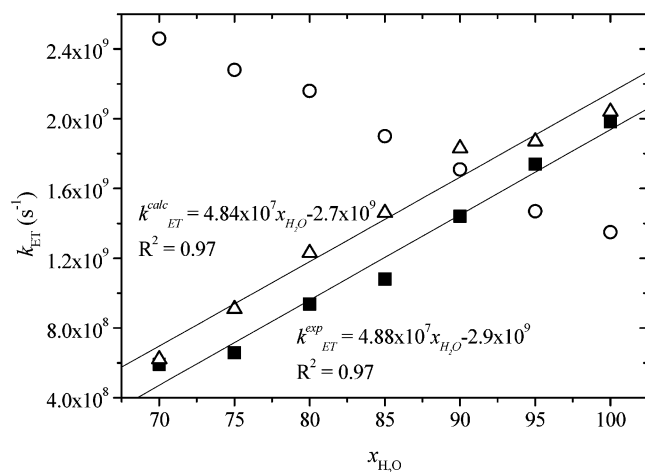


**Figure 10.** Plot of experimental electron-transfer rate constant  $k_{\text{ET}}^{\text{exp}}$  (■) for NAYA in dioxane–water mixtures from 70% (v/v) water concentration to pure water shows an increase with increasing water concentration.  $k_{\text{ET}}^{\text{calc}}$  (○) calculated using Marcus's relation and the Born equation showed an inverse profile of  $k_{\text{ET}}$  with increasing water concentration. The calculated electron-transfer rate constant  $k_{\text{ET}}^{\text{calc}}$  (△) using Seidel's solvent correction shows good agreement with the experimental  $k_{\text{ET}}^{\text{exp}}$ .

measured variation of the correction term  $\Delta G(\epsilon)$  from DMF to water.<sup>19</sup> This is not surprising given the limitations of the Born equation, which does not take into account, for example, hydrogen bonds. A value of  $\Delta G(\epsilon) = -0.1$  eV was calculated by Seidel et al. using eq 33 while the experimental data pointed to a much larger variation of  $\Delta G(\epsilon) = -0.71$  eV.<sup>35</sup>

Therefore, in an attempt to carry out a crude estimate of the variation of  $\Delta G(\epsilon)$  in the polarity range of 70–100% water ( $54 < \epsilon < 78.4$ ), we parametrized eq 33 in order to fit  $\Delta G(\epsilon) = -0.71$  eV to a variation of the dielectric constant from 37 (DMF or AN) to 78.4 (water). Specifically,  $\Delta G(\epsilon)$  values from eq 30 were multiplied by a factor of 0.71/0.1. With this parametrization, the calculated values of the free energy of electron transfer ranged from  $\Delta G^\circ = -0.32$  eV ( $-7.4$  kcal/mol), in the 30:70 dioxane water mixture, to  $\Delta G^\circ = -0.47$  eV ( $-10.8$  kcal/mol) in water.

Values of the electron-transfer rate constant in the dioxane–water mixtures were calculated using eq 34

$$k_{\text{ET}} = \frac{2\pi}{\hbar} \frac{|V(r)|^2}{(4\pi k_{\text{B}} T \lambda)^{1/2}} \exp(-\Delta G^\ddagger/k_{\text{B}} T) \quad (34)$$

where  $\Delta G^\ddagger$  is given by eq 31, in which  $\lambda$  is evaluated with eq 35

$$\lambda = \frac{\Delta e^2}{4\pi\epsilon_0} \left( \frac{1}{r_{\text{ion}}} - \frac{1}{a_{\text{EC}}} \right) \left( \frac{1}{(n_{\text{D}})^2} - \frac{1}{\epsilon_{\text{W}}} \right) \quad (35)$$

Figure 10 shows the profile of calculated and experimental values of the electron-transfer rate constants  $k_{\text{ET}}$  as a function of increasing water concentration in dioxane–water mixtures. It is evident from Figure 10 that the values of  $k_{\text{ET}}$  calculated using Seidel's correction for the activation energy is in excellent agreement with the experimental values of  $k_{\text{ET}}$ , whereas the calculated  $k_{\text{ET}}$  values using the Born approximation (eq 33) fail to even reproduce the correct trend with increasing water concentration.

A calculation of the electronic coupling matrix element resulted in a value of 21.2 meV, considerably superior to the values reported in the literature of 0.3 meV.<sup>27</sup>

**Prediction of Double-Exponential Decays and Interpretation of Proteins Fluorescence.** On the basis of the foregoing kinetic analysis of results, it is clear that experimental observation of double-exponential decays with NAYA depends on three factors: the ground-state population of rotamers, solvent viscosity, and solvent polarity. In relation to the rotamer population, simulations using the present kinetic model show that increasing the population of quenched conformer (increasing  $k_{\text{r}}$  with respect to  $k_{\text{r}'}$ ) strongly increases the double-exponential nature of the decay, while the opposite leads to single-exponential decays. The value of the molar fraction of the nonquenched conformer in dioxane from <sup>1</sup>H NMR ( $\alpha = 0.46$ ) suggests that hydrophobic environments may favor this conformer, hence, leading to single-exponential decays. However, the appearance of a single-exponential decay in nonpolar mediums is essentially due to the decrease of the electron-transfer rate constant.

Second, increasing solvent viscosity (i.e., decreasing both  $k_{\text{r}}$  and  $k_{\text{r}'}$  with respect to  $k_{\text{ET}}$ ) also increases the double-exponential nature of the decay, up to the limit of slow exchange. Finally, increasing solvent polarity (i.e., increasing  $k_{\text{ET}}$  with respect to both  $k_{\text{r}}$  and  $k_{\text{r}'}$ ) obviously produces the same result. This effect is evident in the fluorescence decays in dioxane–water mixtures, where, only for a polarity larger than that of the 70% v/v water mixture, double exponentials were observed (Figure 4). The relative dielectric constant of this mixture has a value ca. 55 (Table 4), which corresponds to a  $k_{\text{ET}}$  value around  $6 \times 10^8$  s<sup>-1</sup>. The observation of single-exponential decays of NAYA in methanol, acetonitrile, and dimethyl sulfoxide (Table 1) is thus explained by an insufficiently high  $k_{\text{ET}}$  with respect to the rotational constants, which is predicted from the lower dielectric constants and lower excitation energies  $h\nu$  in these solvents (see eqs 22–24). Accordingly, the fluorescence lifetimes of NAYA in the same solvents (Table 1) are, with an exception for DMSO (known for quenching fluorescence), much closer to the lifetimes of tyrosine due to inefficient quenching.

Trifluoroethanol (TFE) is a quite interesting solvent in this respect. Despite its low dielectric constant, the fluorescence decays of NAYA in this solvent are similar to those observed in water. The special feature of TFE is its large hydrogen-bond donor strength, which shifts the absorption spectrum of NAYA to higher energy, thus contributing in turning ET more exothermic. However, the difference in  $h\nu$  with respect to water amounts to only 0.4 kcal/mol, which does not appear to compensate the estimated increase of  $\Delta G^\circ$ , resulting from the decrease of the dielectric constant from water to TFE. The TFE case recalls that great care must be exercised in predicting electron-transfer rate constants.

Despite these precautions, we will quote a last illustrative example of the dramatic effect of the magnitude of  $k_{\text{ET}}$  on the nature of the fluorescence decay of NAYA. Among the various tyrosine analogues studied by Laws et al., all of them that have their  $\alpha$ -carbonyl group blocked show double-exponential decays. However, Haas et al.<sup>6</sup> measured *N*-acetyltyrosine-*N'*-methylamide and obtained a single-exponential decay in water at room temperature. We also obtained a single-exponential decay with this compound in the same conditions (2.3 ns) and searched for the reason of this difference from NAYA. The electron affinity calculated for the amide and methylamide peptides showed a decrease of 4.8 kcal/mol (from 5.9 to 1.1 kcal/mol), suggesting that methyl substitution would make the peptide less prompt to accept electrons. Actually, this difference causes a 1 order of magnitude decrease on the calculated  $k_{\text{ET}}$  (from  $2 \times 10^9$  s<sup>-1</sup> to  $1.8 \times 10^8$  s<sup>-1</sup>), which leads to prediction of a single-exponential decay as experimentally observed.

In conclusion, observation of double- or single-exponential decays with NAYA depends on a delicate balance between the rates of rotamer interchange and the intramolecular electron-transfer rate constant, which in turn depend on solvent (viscosity and polarity) and temperature.

As an application to interpretation of tyrosines' fluorescence in proteins, the present model permits prediction of a limited number of situations in which observation of double-exponential decays should occur. For example, a water-exposed tyrosine should present a double-exponential decay at room temperature because polarity should be waterlike and viscosity should be equal or higher than water's. On the contrary, a buried tyrosine within a protein is predicted to decay as a single-exponential, in absence of phenomena other than the intramolecular electron transfer, because the dielectric constant will be too low and consequently so will  $k_{ET}$ . Furthermore, the kinetic analysis of single tyrosine decay permits extraction of some information on the viscosity ( $k_f$  and  $k_r$ ) and polarity ( $k_{ET}$ ) of the environment of that tyrosine within the protein.

### Conclusion

The present work shows strong evidence that the nature of the fluorescence decays (single- or double-exponential) of the model compound of tyrosine within a protein, NAYA, depends on three factors: the population of rotamers in the ground state (ca.  $1/3$  in the case of NAYA in water), the medium polarity, and the medium viscosity, which in turn depend on temperature. The results have been globally accounted for with a kinetic model in which interconversion of the rotamers on the nano-second time scale is considered. A set of equations that can be used to predict the nature or analyze the fluorescence decays of tyrosines in proteins, in the absence of other quenching processes, is presented. Thus, the proposed kinetic model may be helpful in elucidating not yet explained features of tyrosines' fluorescence in proteins.

**Acknowledgment.** This work was supported by Fundação para a Ciência e Tecnologia (FCT), Portugal (POCTI/3513/BME/2000). M.N. thanks the FCT for the Ph.D. Grant SRFH/BD/9096/2002.

### References and Notes

- (1) Cowgill, R. *Biochemical Fluorescence: Concepts*; Chen, R. F., Edelho, H., Eds.; Marcel Dekker: New York, 1976; Vol. 2, pp 441–487.
- (2) Ross, J. B. A.; Laws, W. R.; Rousslang, K. W.; Wyssbrod, H. R. *Topics in Fluorescence Spectroscopy, Biochemical Applications*; Lakowicz, J. R., Ed.; Plenum Press: New York, 1992; Vol. 3, pp 1–63.
- (3) Lee, J.; Ross, R. T.; Thampi, S.; Leurgans, S. *J. Phys. Chem.* **1992**, *96*, 9158–9162.
- (4) Laws, W. R.; Ross, J. B. A.; Wyssbrod, H. R.; Beechem, J. M.; Brand, L.; Sutherland, J. C. *Biochemistry* **1986**, *25*, 599–607.
- (5) Laws, W. R.; Ross, J. B. A.; Buku, A.; Sutherland, J. C.; Wyssbrod, H. R. *Biochemistry* **1986**, *25*, 607–612.
- (6) Haas, E.; Montelione, G. T.; McWherter, C. A.; Scheraga, H. A. *Biochemistry* **1987**, *26*, 1672–1683.
- (7) Libertini, L. J.; Small, E. W. *Biophys. J.* **1985**, *47*, 765–772.
- (8) Gauduchon, P.; Wahl, Ph. *Biophys. Chem.* **1978**, *8*, 87–104.
- (9) Applewhite, T. H.; Niemann, C. *J. Am. Chem. Soc.* **1959**, *81*, 2208–2213.
- (10) Murov, S. L.; Carmichael, I.; Hug, G. L. *Handbook of Photochemistry*, 2nd ed.; Marcel Dekker: New York, 1993.
- (11) Giestas, L.; Yihwa, C.; Lima, J. C.; Vantier-Giongo, C.; Lopes, A.; Maçanita, A. L.; Quina, F. H. *J. Phys. Chem. A* **2003**, *107*, 3263–3269.
- (12) Striker, G.; Subramaniam, V.; Seidel, C. A. M.; Volkmer, A. J. *J. Phys. Chem. B* **1999**, *103*, 8612–8617.
- (13) Melo, E. C.; Costa, S. M. B.; Maçanita, A. L.; Santos, H. J. *Colloid Interface Sci.* **1991**, *141*, 439–453.
- (14) Varela, A. P.; da Graça Miguel, M.; Burrows, H.; Maçanita, A. L.; Becker, R. S. *J. Phys. Chem.* **1995**, *99*, 16093–16100.
- (15) Ross, R. T.; Lee, J. *J. Phys. Chem. B* **1998**, *102*, 4612–4618.
- (16) Tourmon, J. E.; Kuntz, E.; ElBayoumi, M. A. *Photochem. Photobiol.* **1972**, *16*, 425–433.
- (17) Selim, E. T. M.; Fahmey, M. A.; Ghonime, H. S. *Indian J. Phys.* **1991**, *65*, 171.
- (18) Zachariasse, K., Thesis, Free University of Amsterdam, 1972.
- (19) Seidel, C.; Orth, A.; Greulich, K.-O. *Photochem. Photobiol.* **1993**, *58*, 178–184.
- (20) The calculated atomic charge of the phenol oxygen is reduced from  $-0.259$  in the ground state to  $-0.224$  in the excited state.
- (21) Moreira, P. F., Jr.; Giestas, L.; Yihwa, C.; Vantier-Giongo, C.; Quina, F. H.; Maçanita, A. L.; Lima, J. C. *J. Phys. Chem. A* **2003**, *107*, 4203–4210.
- (22) Tolbert, L. M.; Solntsev, K. M. *Acc. Chem. Res.* **2002**, *35*, 19–27.
- (23) Solntsev, K. M.; Huppert, D.; Agmon, N. *J. Phys. Chem. A* **1999**, *103*, 6984–6997.
- (24) Willis, K. J.; Szabo, A. G. *J. Phys. Chem.* **1991**, *95*, 1585–1589.
- (25) However, tyrosine shows double-exponential decays similar to those of NAYA at low pH, when the higher electron affinity of the protonated carboxyl group allows electron transfer.
- (26) Becker, R. S. *Theory and Interpretation of Fluorescence and Phosphorescence*; Wiley and Sons: New York, 1969.
- (27) Wicz, W.; Rzeska, A.; Lukomska, J.; Stachowiak, K.; Karolczak, J.; Malicka, J.; Lankiewicz, L. *Chem. Phys. Lett.* **2001**, *341*, 99–106.
- (28) Reynders, P.; Dreeskamp, H.; Kühnle, W.; Zachariasse, K. A. *J. Phys. Chem.* **1987**, *91*, 3982–3992.
- (29) Reynders, P.; Kühnle, W.; Zachariasse, K. A. *J. Am. Chem. Soc.* **1990**, *112*, 3929–3939.
- (30) Duvencek, G., Ph.D. Thesis, Georg-August-Universität, Göttingen, 1986.
- (31) Costa, S. M.; Maçanita, A. L.; Formosinho, S. J. *J. Phys. Chem.* **1984**, *88*, 4089–4095.
- (32) Rehm, D.; Weller, A. *Isr. J. Chem.* **1970**, *8*, 259–271.
- (33) Seidel, C. A. M.; Schulz, A.; Sauer, M. H. M. *J. Phys. Chem.* **1996**, *100*, 5541–5553.
- (34) Weller, A. *Z. Phys. Chem. N. F.* **1982**, *133*, 93–98.
- (35) Siedel et al. showed from quenching experiments of fluorescent dyes by nucleobases<sup>33</sup> and for quenching of coumarins<sup>36</sup> by nucleotides in DMF and water that  $\Delta G(\epsilon)$  is in the order of  $-0.5$  to  $-0.9$  eV. This range was narrowed to a value of  $-0.71$  eV on the basis of the change in acidity from cresol ( $pK_a = 10$ ) to the respective radical cation ( $pK_a = -2$ ).
- (36) Seidel, C. *Proc. SPIE-Int. Soc. Opt. Eng.* **1991**, *1432*, 91–104.